Pergamon

Int. J. Heat Mass Transfer. Vol. 38, No. 14, pp. 2539–2548, 1995
Copyright © 1995 Elsevier Science Ltd
Printed in Great Britain. All rights reserved
0017–9310/95 $9.50+0.00

0017–9310(95)00016–X

Numerical simulations of interface viscosity effects on thermoconvective motion in two-dimensional rectangular boxes

V. C. REGNIER, P. M. PARMENTIER, G. LEBON†
University of Liège, Institute of Physics, B-5, B-4000 Liège, Belgium

and

J. K. PLATTEN
University of Mons, Faculty of Medecine, Place du Parc, B-7000 Mons, Belgium

(*Received for publication in final form* 16 *December* 1994)

Abstract—In thermoconvection problems, it is generally assumed that the dissipative effects at the interface play a negligible role. In dimensionless form, the importance of this effect can be quantified by the interface viscosity number *Vi*. The purpose of this paper is to examine the effects of an interface viscosity on convective motions through two illustrative situations performed within a two-dimensional (2D) finite-difference code. In the first example, the upper fluid is passive while in the second example, one considers two superposed immiscible fluids in a closed rectangular cavity. The maximum surface velocity, the stream lines and the kinetic energy of the bulk flow are calculated for *Vi*-values varying between 0 and 10. For $Vi \geqslant 1$, it is shown that the interface viscosity has a non-negligible influence, particularly in the vicinity of the interface.

1. INTRODUCTION

The purpose of the present paper is to show the effects resulting from the presence of an interface viscosity on thermoconvective motions. Physical arguments in support of the existence of a surface viscosity were presented among others by Davies and Rideal [1], Bedeaux [2], Bedeaux *et al.* [3], Goodrich [4], Sorensen [5] and Edwards *et al.* [6].

The role of an interface viscosity in thermoconvection was studied by Scriven [7] and Scriven and Sternling [8]. By performing a linear stability analysis, Scriven and Sternling [8] showed that surface viscosity inhibits stationary instability in a thin layer of fluid submitted to a vertical temperature gradient.

In parallel with Scriven and Sternling's works, experimental observations led Cardin and Nataf [9] and Cardin *et al.* [10] to conclude the existence of the interface viscosity. The same authors and Wahal and Bose [11] also propose a linear study of stability of two immiscible fluid layers heated from below, from which it follows that an interface viscosity reinforces the stability while the nature of the most unstable eigenmode changes from stationary to oscillatory. The influence of an interfacial viscosity on thermoconvective instability was also examined by Gousbet *et al.* [12, 13].

Experimental observations have confirmed that surface viscosity may be important for some liquid surfaces supporting thin active films like silicone oils over glycerol layers [1, 9, 14] or long-chain alcohol films like heptanol, tetradecanol or hexadecanol [15].

In this note, the influence of interface viscosity in thermoconvection is examined through two simple applications selected in order that interface viscosity effects are not masked by other phenomena. The first application concerns a single liquid layer whose upper boundary is in contact with an ambient gas. The liquid is submitted to a temperature gradient respectively vertical and horizontal; convection sets in under the combined effects of buoyancy forces (Rayleigh–Bénard effect) and variations of the surface tension with the temperature (Marangoni effect). When the temperature gradient is vertical, convection appears after the temperature difference between the lower and upper faces has reached a critical value while under a horizontal temperature gradient, the fluid is immediately in motion. In the second application, one considers two immiscible liquid layers subject to a horizontal temperature gradient: the two liquids are confined in a rectangular box, the coupled Rayleigh–

†Also at Louvain University, Louvain-la-Neuve, Department of Mechanics. Author to whom correspondence should be addressed.

NOMENCLATURE

Bi	Biot number, $Bi^{\Sigma} \equiv h^{\Sigma}d^{\Sigma}/k^{\Sigma}$
C_p	specific heat
d	thickness of the layer
K	kinetic energy
g	gravity acceleration
h	thermal surface conductance
k	thermal conductivity
L	width of the box
Ma	Marangoni number, $Ma^{\Sigma} \equiv \gamma^{\Sigma}\beta(d^{\Sigma})^2/\mu^{\Sigma}\kappa^{\Sigma}$
$\mathbf{n}$	normal unit-vector
p	pressure
Pr	Prandtl number, $Pr^{k} \equiv \nu^{k}/\kappa^{k}$
Ra	Rayleigh number, $Ra^{k} \equiv g\alpha^{k}\beta(d^{k})^4/\kappa^{k}\nu^{k}$
S	area
t	time
T	temperature
$\mathbf{u}(u,v,w)$	velocity field vector
Vi	interface viscosity number, $Vi^{\Sigma} \equiv (\eta_s^{\Sigma}+\varepsilon_s^{\Sigma})/\mu^{k=1}d^{k=1}$
x,y,z	Cartesian coordinates.

Greek symbols

α	coefficient of volumic expansion
β	characteristic temperature gradient
ε_s	surface shear viscosity
$\gamma(>0)$	rate of change of surface tension
η_s	coefficient of dilatational viscosity
κ	thermal diffusivity
μ	dynamic viscosity
ν	kinematic viscosity
ρ	density
σ	surface tension
ω	vorticity
ψ	stream line function.

Subscript

0	reference state.

Superscripts

$k(=1,2)$	integer referring to the fluid layer
$\Sigma(=1,2)$	integer referring to the interface.

Bénard and Marangoni effects are still acting. Numerically, a 2D finite-difference code is used.

2. MATHEMATICAL FORMULATION

Consider the general configuration formed by two immiscible fluids 1 and 2, of thicknesses d^1 and d^2, respectively, in a 3D rectangular cavity of width L (see Fig. 1). Orientations of the x and y axes are given by Fig. 1, the z-axis is normal to the picture. The fluids are supposed to be of infinite horizontal extent in the z-direction. For numerical facilities, it is assumed that both the interface and the upper surface are flat. The fluids are Newtonian with densities given by the state equations

$$\rho^{k} = \rho_0^{k}(1-\alpha^{k}(T^{k}-T_0^{k})) \tag{1}$$

superscript k refers to the layer (k = 1, 2), ρ_0^{k} is the density at temperature T_0^{k}, α^{k} the constant coefficient of volumic expansion. Boussinesq's approximation is taken for granted: accordingly, the dynamic viscosity μ^{k}, the specific heat C_p^{k}, and the thermal conductivity k^{k} are constant while the rate of production of heat by internal friction is negligibly small.

The interfaces, referred to by the superscript Σ (Σ = 1 refers to the interface between fluid 1 and fluid

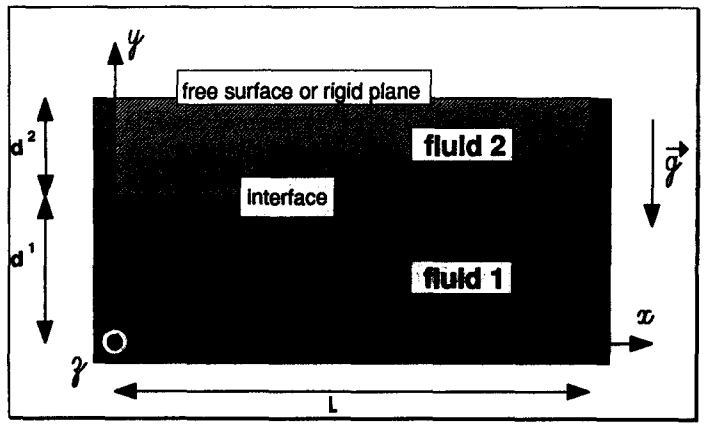

Fig. 1. The geometrical configuration.

2; $\Sigma = 2$ refers to the free surface), are submitted to a surface tension σ^Σ whose equation of state is

$$\sigma^\Sigma = \sigma_0^\Sigma - \gamma^\Sigma (T^\Sigma - T_0^\Sigma) \tag{2}$$

where σ_0^Σ is the surface tension at temperature T_0^Σ, γ^Σ the constant rate of change of surface tension with temperature, is supposed to be positive.

According to Scriven [7], the local form of the momentum balance equation at the non-deformable interface is given by

$$\mu^1 \frac{\partial w^1}{\partial y} - \mu^2 \frac{\partial w^2}{\partial y} = \frac{\partial \sigma}{\partial z} + (\eta_s + \varepsilon_s) \times \frac{\partial}{\partial z}\left(\frac{\partial u}{\partial x} + \frac{\partial w}{\partial z}\right) + \varepsilon_s \frac{\partial}{\partial x}\left(\frac{\partial w}{\partial x} - \frac{\partial u}{\partial z}\right) \tag{3}$$

$$\mu^1 \frac{\partial u^1}{\partial y} - \mu^2 \frac{\partial u^2}{\partial y} = \frac{\partial \sigma}{\partial x} + (\eta_s + \varepsilon_s) \times \frac{\partial}{\partial x}\left(\frac{\partial u}{\partial x} + \frac{\partial w}{\partial z}\right) + \varepsilon_s \frac{\partial}{\partial z}\left(\frac{\partial u}{\partial z} - \frac{\partial w}{\partial x}\right) \tag{4}$$

after assuming that the interface density is sufficiently small to neglect inertial and gravitational effects. Superscripts 1 and 2 refer to the two fluids located at each side of the interface, a quantity without any superscript means a quantity evaluated at the interface. From now on, the analysis will be restricted to a 2D system, so that the interface reduces to a 1-D line.

For convenience, the variables are expressed in dimensionless form. Distances are scaled by the thickness of the bottom layer d^1; the velocity vector $\mathbf{u} = (u, v)$, time t, pressure p, temperature and surface tension σ^Σ are scaled by κ^1/d^1, $(d^1)^2/\kappa^1$, $\kappa^1 \nu^1 \rho_0^1/(d^1)^2$, βd^1 and σ_0^Σ respectively

Finally, the relevant balance equations in the two layers are (k = 1, 2):

$$\frac{\partial u^k}{\partial x} + \frac{\partial v^k}{\partial y} = 0 \quad \text{(continuity equation)} \tag{5}$$

$$\frac{\partial u^k}{\partial t} + u^k \frac{\partial u^k}{\partial x} + v^k \frac{\partial u^k}{\partial y} = Pr^k \times \left(\frac{\kappa^k}{\kappa^1}\frac{\mu^1}{\mu^k}\frac{\partial p^k}{\partial x} + \frac{\kappa^2}{\kappa^1}\left(\frac{\partial^2 u^k}{\partial x^2} + \frac{\partial^2 u^k}{\partial y^2}\right)\right) \tag{6}$$

$$\frac{\partial v^k}{\partial t} + u^k \frac{\partial v^k}{\partial x} + v^k \frac{\partial v^k}{\partial y} = Pr^k\left(\frac{\kappa^k}{\kappa^1}\frac{\mu^1}{\mu^k}\frac{\partial p^k}{\partial y} + \frac{Pr^1}{Pr^k}\frac{\alpha^k}{\alpha^1} Ra^k T^k + \frac{\kappa^k}{\kappa^1}\left(\frac{\partial^2 v^k}{\partial x^2} + \frac{\partial^2 v^k}{\partial y^2}\right)\right) \quad \text{(Navier–Stokes equations)} \tag{7}$$

$$\frac{\partial T^k}{\partial t} + u^k \frac{\partial T^k}{\partial x} + v^k \frac{\partial T^k}{\partial y} = \frac{\kappa^k}{\kappa^1}\left(\frac{\partial^2 T^k}{\partial x^2} + \frac{\partial^2 T^k}{\partial y^2}\right) \quad \text{(temperature equation)}. \tag{8}$$

The boundary conditions corresponding to each particular case studied in this note will be specified at the end of the present section.

To eliminate the pressure term which has a destabilizing numerical effect, one transforms the balance equations (5)–(8) in a vorticity-stream line representation by setting

$$u^k = \frac{\partial \Psi^k}{\partial y} \quad v^k = -\frac{\partial \Psi^k}{\partial x} \quad \omega^k = \frac{\partial u^k}{\partial y} - \frac{\partial v^k}{\partial x}. \tag{9}$$

Ψ^k is the stream line function and ω^k the vorticity; in terms of Ψ^k and ω^k, the balance equations (5)–(8) read as

$$\frac{\partial \omega^k}{\partial t} + \frac{\partial}{\partial x}\left(\frac{\partial \Psi^k}{\partial y}\omega^k + Pr^1 \frac{\alpha^k}{\alpha^1} Ra^k T^k\right) + \frac{\partial}{\partial y}\left(-\frac{\partial \Psi^k}{\partial x}\omega^k\right) - Pr^k \frac{\kappa^k}{\kappa^1}\left(\frac{\partial^2 \omega^k}{\partial x^2} + \frac{\partial^2 \omega^k}{\partial y^2}\right) = 0 \tag{10}$$

$$\frac{\partial T^k}{\partial t} + \frac{\partial}{\partial x}\left(\frac{\partial \Psi^k}{\partial y} T^k\right) + \frac{\partial}{\partial y}\left(-\frac{\partial \Psi^k}{\partial x} T^k\right) - \frac{\kappa^k}{\kappa^1}\left(\frac{\partial^2 T^k}{\partial x^2} + \frac{\partial^2 T^k}{\partial y^2}\right) = 0 \tag{11}$$

$$\frac{\partial^2 \Psi^k}{\partial x^2} + \frac{\partial^2 \Psi^k}{\partial y^2} = \omega. \tag{12}$$

The system (10)–(12) is solved by a semi-implicit finite-difference ADI (Alternating Direction Implicit) scheme. The time is used as the iterative parameter so that the scheme is pseudo-unsteady.

To illustrate the influence of the interface viscosity on thermoconvective motions, two situations are analyzed. Firstly, the upper fluid is passive so that the interface can be considered as a liquid–gas interface. The liquid is contained in an open rectangular box of infinite extension in the z-direction and its free surface is submitted to a temperature-dependent surface tension. The layer is subject to a horizontal and a vertical temperature gradient, respectively.

In the case of a horizontal heating, a thermoconvective motion is instantaneously induced; there is no quiescent reference state contrary to what happens with a vertical temperature gradient. The physical parameters are in this problem given by $Pr = 1000$, $Ra = 2000$, $Ma = 100$, which corresponds to a silicon oil layer of one centimeter thick subject to a temperature difference of 1°C.

In presence of a vertical temperature gradient the dimensionless numbers are $Pr = 7$, $Ra = 10\,000$, $Ma = 1000$, corresponding to a water layer of 2 cm thick with a temperature difference of 0.1°C. The critical values of the Marangoni and Rayleigh numbers obtained for an unbounded horizontal layer [16] are $Ma^c \cong 50$ and $Ra^c \cong 500$.

The corresponding boundary conditions are:

on the vertical walls:

$$u = 0 \quad v = 0 \quad \text{(no-slip condition)} \tag{13}$$

on the lower wall:

$$u = 0 \quad v = 0 \quad \text{(no-slip condition)} \tag{14}$$

on the free upper surface:

$$\frac{\partial u}{\partial y} = -Ma\frac{\partial T}{\partial x} + Vi\frac{\partial^2 u}{\partial x^2} \quad \text{(Marangoni condition)} \tag{15}$$

$$v = 0 \quad \text{(flat surface)}. \tag{16}$$

The conditions are valid for both situations, namely a vertical and a horizontal temperature gradient; in the latter case the vertical walls are assumed perfectly heat conducting with

$$T = 0.5 \text{ at } x = 0 \quad T = -0.5 \text{ at } x = L/d \tag{17}$$

while the temperature field at the horizontal walls is given by [14–16]

$$T = 0.5 - x/(L/d). \tag{18}$$

In the case of vertical temperature gradient, the vertical walls are supposed to be adiabatically isolated:

$$\frac{\partial T}{\partial x} = 0 \tag{19}$$

and the rigid lower wall is perfectly conducting with

$$T = 0.5. \tag{20}$$

finally the upper free surface is modelled by the Newton cooling law:

$$\frac{\partial T}{\partial y} + Bi(T + 0.5) = 0. \tag{21}$$

In the second problem, we consider two immiscible fluids in a closed rectangular cavity submitted to a horizontal temperature gradient. The physical properties of the fluids are the same for fluids 1 and 2 except for the density ($\rho^1 = 2\rho^2$). The dimensionless parameters characterizing the fluids are $Pr^1 = 1$, $Pr^2 = 2$, $Ra^1 = 2500$, $Ma = 100$, $L/d^1 = 4$, $d^2/d^1 = 1$, $\mu^2/\mu^1 = 1$, $\alpha^2/\alpha^1 = 1$, $k^2/k^1 = 1$, $\kappa^2/\kappa^1 = 1$. It results from these values that $Ra^2 = 1250$.

The relevant boundary conditions are:
on the vertical walls:

$$u = 0 \quad v = 0 \tag{22}$$

$$T = -0.5 \text{ at } x = 0 \text{ and } T = 0.5 \text{ at } x = L/d^1 \tag{23}$$

on the horizontal walls:

$$u = 0 \quad v = 0 \tag{24}$$

$$T = x/(L/d^1) - 0.5 \tag{25}$$

on the interface:

$$u^1 = u^2, \quad \text{(velocity continuity)} \tag{26}$$

$$v^1 = v^2 = 0, \quad \text{(flat interface)} \tag{27}$$

$$\frac{\partial u^1}{\partial y} - \frac{\mu^2}{\mu^1}\frac{\partial u^2}{\partial y} = -Ma\frac{\partial T}{\partial x} + Vi\frac{\partial^2 u}{\partial x^2} \quad \text{(Marangoni condition)} \tag{28}$$

$$\frac{\partial T^1}{\partial y} = \frac{k^2}{k^1}\frac{\partial T^2}{\partial y} \quad \text{(heat flux continuity)}. \tag{29}$$

A (21×81) grid was used to solve the first problem and a $((21+21) \times 81)$ grid for the second application; the numerical calculations were performed on a 6000/550 RISK IBM workstation. The CPU time per iteration is about 0.5 s and the program requires about 1500 iterations to obtain a stationary solution.

3. RESULTS

For each problem, we have determined the influence of an interface viscosity on the steady flow for a range of Vi-values running from 0 to 10. For $Vi \ll 1$, no quantitative difference with respect to the case $Vi = 0$ has been noticed. For $Vi \gg 10$, the interface is strongly viscous and can be viewed as a rigid plane within the limit $Vi \to \infty$.

3.1. *One single layer*

When the temperature gradient is horizontal, the motion takes the form of a single cell (Fig. 2). When the temperature gradient exceeds a critical value depending on the characteristics of the fluid, the cell becomes unstable and breaks into smaller cells [17–19], but this situation will not be treated in the present study. In Fig. 2 are represented the iso-stream lines corresponding to different surface viscosities ($Vi = 0$, 1, 10 and ∞). The aspect ratio is fixed equal to 4. Even for $Vi = 0$, the centre of the vortex is not situated exactly at the middle of the box because of the presence of surface tensions (Marangoni effect). When this effect is reduced due to the presence of a surface viscosity, the cell becomes more and more symetric and is perfectly symmetric for $Vi = \infty$, as expected.

An interesting parameter characterizing the flow is the dimensionless kinetic energy per unit-volume

$$K = \frac{(d^1)^2}{L\sum_{j=1}^{n} d^j}\sum_{j=1}^{n}\frac{\rho_0^j}{\rho_0^1}\int\int \mathbf{u}^j \cdot \mathbf{u}^j \, dS^j \tag{30}$$

and the maximum surface velocity (u_T^{max}), n is the number of fluid layers and S^j the surface of fluid j. The quantities K and u_T^{max} are calculated for various surface viscosities ($Vi = 0$, 1, 10 and ∞) and aspect ratios ($L/d = 1$, 2, 4, 6 and 10) (see Table 1).

For a fixed surface viscosity, the variation of the aspect ratio produces two antagonist effects: firstly, when the aspect ratio increases, the temperature gradient decreases and induces a decrease of the energy per unit-volume. Secondly, for small values of L/d, the

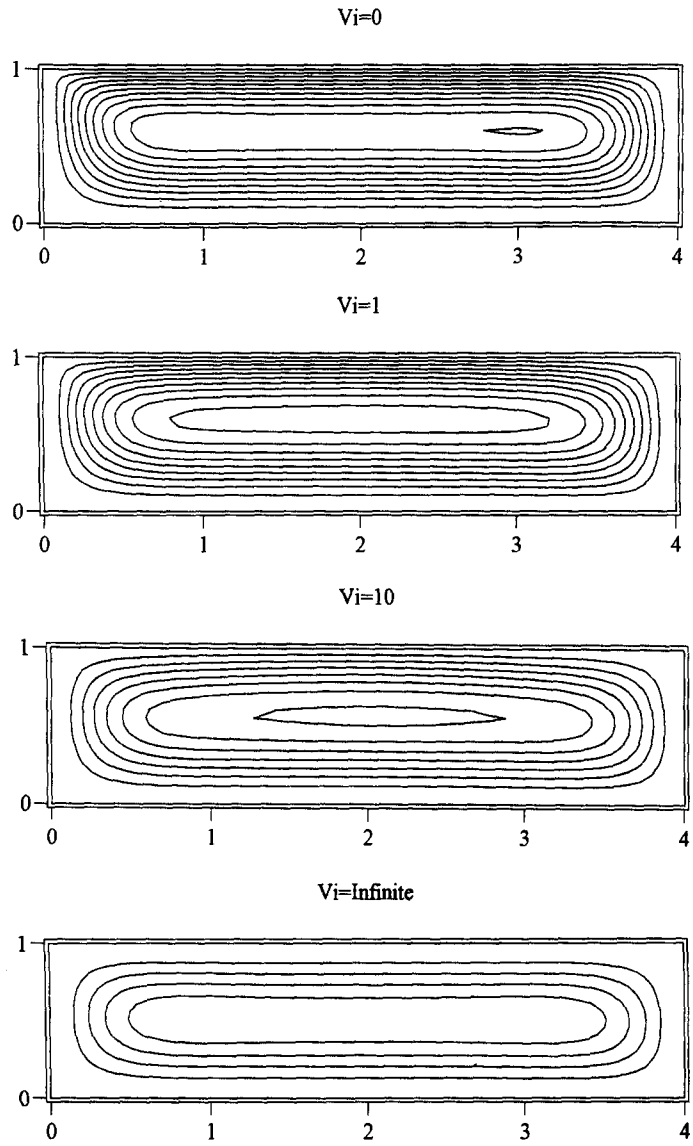

Fig. 2. Iso-stream lines in a single layer subject to a horizontal temperature gradient, $Vi = 0, 1, 10, \infty$, $Pr = 1000$, $Ra = 2000$, $Ma = 100$.

wall effects become dominant and the dissipative effects due to the presence of a surface viscosity are more important. This is a consequence of the large values taken by the term $\partial^2 u/\partial x^2$ in equation (15). The first effect is mainly responsible for the decrease of the kinetic energy and the maximum surface velocity when L/d is growing at the condition that the surface viscosity remains small ($Vi \leqslant 1$); on the contrary, for large Vi-values the second effect becomes dominant and produces an increase of the velocity at the surface.

The decrease of the kinetic energy and the maximum surface velocity with respect to the surface

Table 1. The kinetic energy per unit-volume and the maximum surface velocity as a function of the viscosity number, Vi, and the aspect ratio, L/d (horizontal temperature gradients)

		L/d = 1		2		4		6		10	
		K	u_T^{max}	K	u_T^{max}	K	u_T^{max}	K	u_T^{max}	K	u_T^{max}
Vi	0	49.80	18.52	47.18	15.11	31.40	11.79	20.49	9.39	9.77	6.35
	1	28.68	9.35	34.05	12.11	26.19	10.94	18.06	8.93	9.06	6.22
	10	19.15	1.08	16.83	3.85	13.03	6.25	10.53	6.67	6.51	3.57
	∞	18.33	0	13.25	0	5.83	0	3.04	0	1.20	0

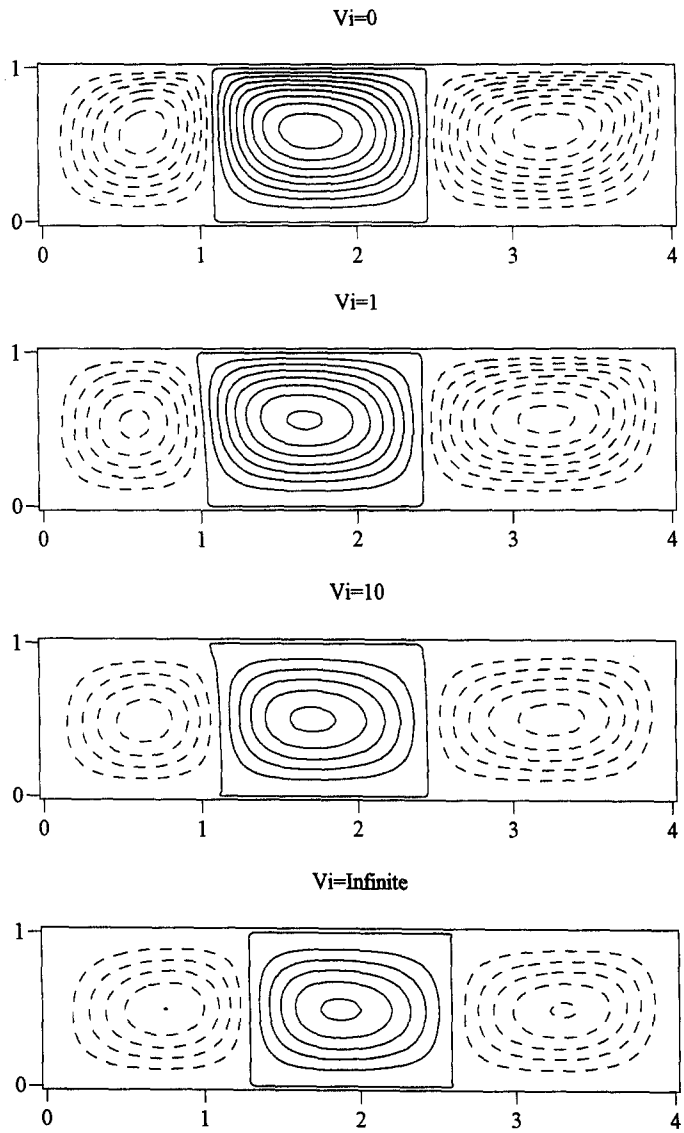

Fig. 3. Iso-stream lines in a single layer subject to vertical temperature gradient, $Vi = 0, 1, 10, \infty$, $Pr = 7$, $Ra = 10\,000$, $Ma = 1000$, $Bi = 1$. Concentric continuous stream lines indicate an anti-clockwise cell while dashed stream lines indicate a clockwise cell.

viscosity depends strongly on the aspect ratio. Indeed the larger the box, the smaller the second derivative of the surface velocity and the smaller the influence of the surface viscosity.

In the presence of a vertical temperature gradient, six stable steady solutions have been found for $L/d = 4$: they consist of two, three or four cells with either a rising or a downward fluid motion along the vertical walls, depending on the initial values of the (Ψ, ω, T) fields. The iso-stream lines for $Vi = 0, 1, 10$ and ∞ are represented in Fig. 3 for the particular case of three cells. When Vi is increased, the density of stream lines decreases, indicating a lowering decrease of the velocity. This result generalizes earlier observations by Scriven and Sternling [8] and Gousbet *et al.* [12, 13], accordingly surface viscosity inhibits the onset of motion in pure Marangoni convection. The centre of the vortex moves towards the middle axes $y = 0.5$; when $Vi = \infty$, the stream lines have $y = 0.5$ as symmetry axis. In Fig. 4 is shown the variation of the dimensionless kinetic energy per unit-volume K vs the surface viscosity. The surface viscosity has a dissipative effect on the kinetic energy; this effect is the most important for small values of Vi. It is worth noticing that the importance of the surface viscosity term depends on the surface velocity profile; the greater the number of cells, the greater the influence of the surface viscosity term, as explicitly shown in Fig. 4.

3.2. *Two immiscible layers*

In the following example, the left wall is colder than the right one. The numerical simulation predicts the emergence of three cells: one anti-clockwise cell in

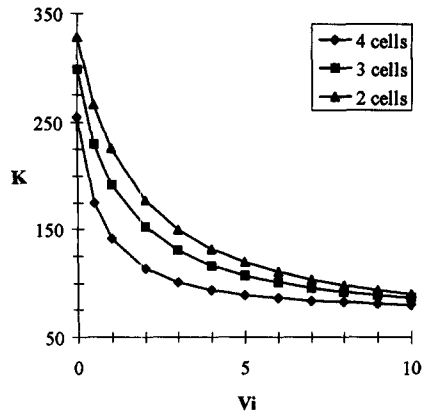

Fig. 4. Variation of the kinetic energy with surface viscosity (single layer with a vertical temperature gradient), $L/d = 4$.

fluid 1, one clockwise cell at the bottom of fluid 2 and one anti-clockwise cell at the top of fluid 2 (see Fig. 5). For small Vi-values, this last cell may split into two anti-clockwise small cells (Fig. 5). The presence of the small middle cell is required to ensure the continuity of velocities; this cell becomes smaller and smaller when Vi is increased. In the limit of $Vi = \infty$, this cell disappears. The sense of rotation of the cells is determined by:

(1) the horizontal temperature gradient: the fluid rises along the hot wall and goes down along the cold wall and

(2) the mechanical coupling at the interface: a non-zero fluid velocity at the interface induces two contra-rotating cells. The sign of the vorticity changes by passing through the interface.

The relative importance of these two mechanisms can be measured by the ratio Ra^2/Ra^1 and the Marangoni number Ma which determines the number of cells to be observed. A 1-D analysis was performed by Villers and Platten [17]; however, in such a study it is impossible to introduce an interface viscosity because the velocity **u** is everywhere constant at the interface, as a direct consequence of their 1-D assumption. The velocity profiles in a monolayer subject to a horizontal temperature gradient has also been studied by differ-

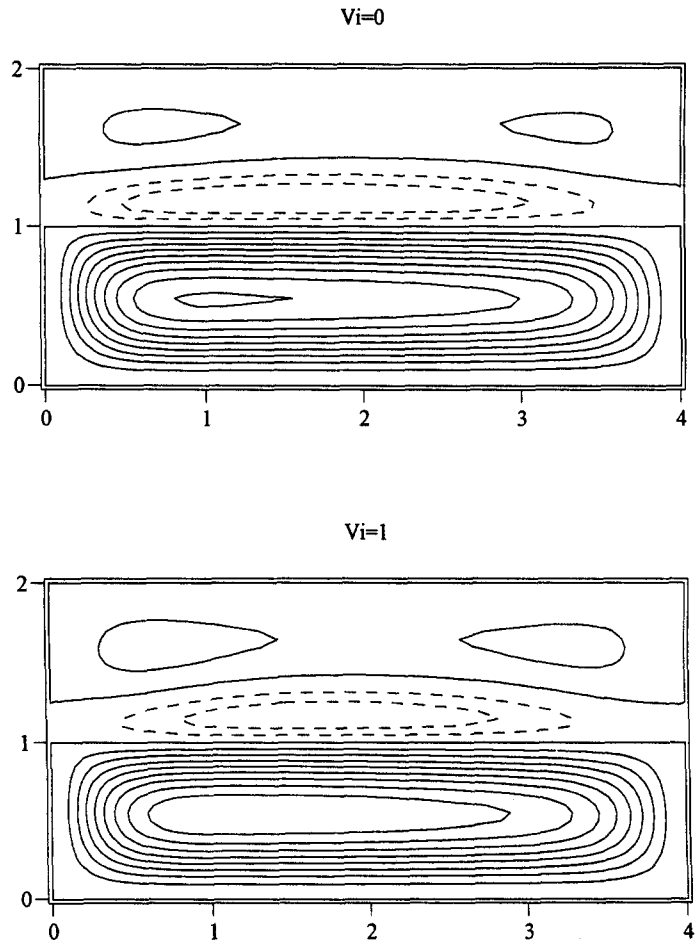

Fig. 5. Iso-stream lines in two layers subject to a horizontal temperature gradient for $Vi = 0, 1, 10, \infty$; $Pr^1 = 1, Pr^2 = 2, Ra^1 = 2500$ ($Ra^2 = 1250$), $Ma = 100, L/d^1 = 4, d^2/d^1 = 1, \mu^2/\mu^1 = 1, \alpha^2/\alpha^1 = 1, k^2/k^1 = 1, \kappa^2/\kappa^1 = 1$. Concentric continuous stream lines indicate an anti-clockwise cell while dashed stream lines indicate a clockwise cell. (*Continued overleaf.*)

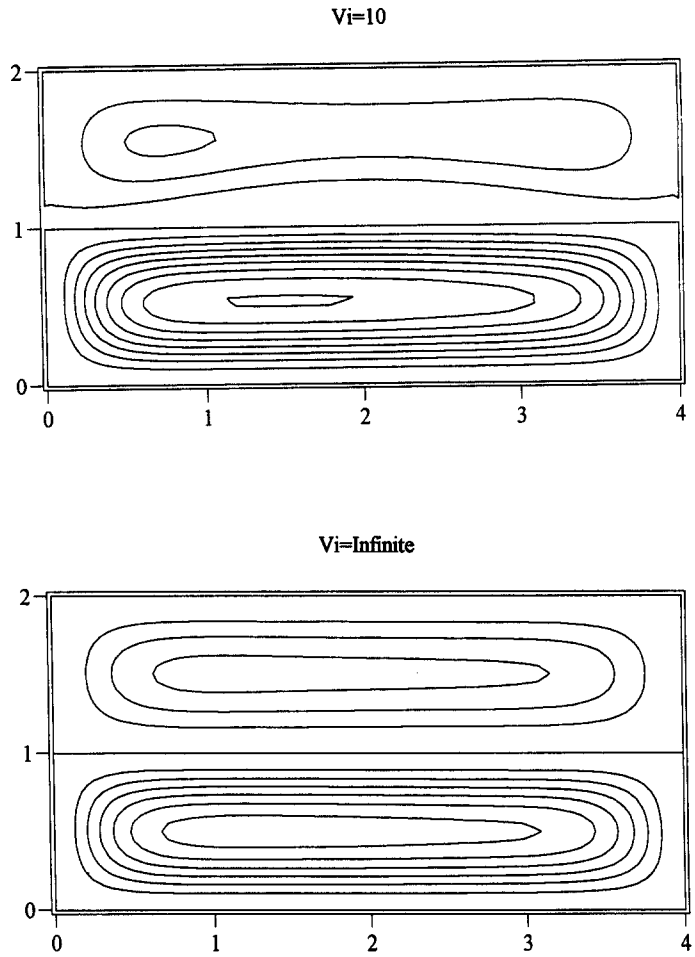

Fig. 5—*continued.*

ent authors (e.g. Kirdyashkin [18] and Parmentier *et al.* [19]).

In the particular case of a rigid interface ($Vi = \infty$), only the first mechanism is relevant and one anticlockwise cell is found in each layer (Fig. 5). When both mechanisms are active, two possibilities are offered:

(1) $Ra^2/Ra^1 \gg 1$ or $Ra^2/Ra^1 \ll 1$: the first mechanism is dominant in the layer with the greatest Rayleigh number. The layer with the smallest Rayleigh number is passive; its motion is mainly caused by the mechanical coupling with the other fluid. One anticlockwise cell will appear in the layer of greater Rayleigh number and one clockwise cell will be generated in the layer of smaller Rayleigh number.

(2) $Ra^2/Ra^1 \approx 1$: the first mechanism has the same importance in both subsystems and induces one anticlockwise cell in each layer. A third clockwise cell will appear in the layer with the smallest Rayleigh number because of the mechanical coupling. The size of this third cell is growing with Ma: when Ma increases, the second mechanism becomes more important.

A numerical simulation has been performed for $Ra^2/Ra^1 = 0.5$ and $Ma = 100$, which corresponds to the second case. For $Vi = 0$, both thermal and mechanical mechanisms act with comparable intensity since the two cells in the upper layer have approximately the same size. Since the interface viscosity reduces the mechanical coupling between both fluids, the clockwise cell in fluid 2 will become smaller and smaller when Vi is increased, as confirmed by Fig. 5.

The variation of the kinetic energy K with the interface viscosity is represented in Fig. 6. The interface viscosity plays an important dissipative role: the kinetic energy has lost 10% of its value at $Vi = 2$ compared with its value at $Vi = 0$. It should also be noticed that the curve slope depends on the aspect ratio of the box. Indeed the larger the box, the smaller the second derivative of the interface velocity and the smaller the influence of the interface viscosity.

4. DISCUSSION AND CONCLUSION

Since the interface is generally considered as a 2-D fluid, it is natural to introduce an interface viscosity in the momentum interface balance equation by analogy

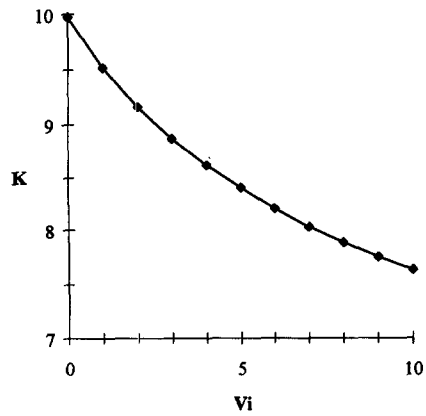

Fig. 6. Variation of the kinetic energy with surface viscosity (two immiscible layers) with a horizontal temperature gradient.

with the shear viscosity appearing in the 3-D momentum equation for the bulk fluid. Clearly, one cannot ignore the effect of this surface viscosity in comparison with the surface tension term without making an approximation and providing a sound justification of this hypothesis. The aim of this note is precisely to discuss the quality of this assumption with respect to the values taken by the so-called viscosity number *Vi*.

In analogy with the classical shear viscosity, the interface viscosity plays a strong dissipative role as exhibited by Figs. 4 and 6. It affects not only the region close to the interface but modifies the bulk fluid motion. The influence of the interface viscosity becomes significant for *Vi*-values larger than unit; it plays a negligible role for $Vi \ll 1$ while for $Vi > 10$, the interface behaves as a rigid one. This particular situation is met either when the interface is covered by unsoluble surfactants which may reduce considerably the interface velocity, or for very thin fluid layers; this is easily understandable because the thickness of the lower layer appears in the denominator of the expression of *Vi* (It is obvious that the term "thin" cannot be given a precise meaning here as the values of η_s and ε_s are not known *a priori*).

As shown in equations (15) and (28), the *Vi*-number is multiplied by the second space derivative of the surface velocity. As a consequence, the surface viscosity effects will depend strongly on the surface velocity profile; in the case of the four-cell structure, the second order derivative of the surface velocity is larger than for three and two cells and this explains why the influence of the surface viscosity is the most important in the four-cell configuration. This is reflected by Fig. 4 where the kinetic energy K is shown to decrease more rapidly in the four-cell pattern. This result was checked to hold true for two-liquid layers where in addition it is observed that K decreases more slowly than for a single fluid layer. It appears thus that interface viscosity effects increase when the number of cells per unit-length along the interface is growing.

Of course, the basic problem is the determination of the interface viscosity *Vi*; one way out would be comparing numerical and experimental experiences. More explicitly, *Vi* could be obtained by measuring the experimental velocity profile and by comparing it with the numerical profiles provided by the present model.

Within the prospect of further applications, we have to point out two important limits of the present analysis. Firstly, the numerical procedure was limited to a 2-D analysis and, secondly, the non-deformability of the interface was not taken into account. Nevertheless, the merit of the above simple model is to open the way to more realistic descriptions and to show explicitly that surface viscosity may have a non-negligible influence on thermoconvective flows.

Acknowledgements—This text presents research of the Belgium program on Interuniversity Poles of Attraction (P.A.I. No. 29) initiated by the Belgian state, Prime Minister's Office, Science Policy Programming. The scientific responsibility is assumed by its authors. This work was also partially supported by the European Communities, Human Capital and Mobility Program under contract ERBCHRXTC 940481.

REFERENCES

1. J. T. Davies and E. K. Rideal, *Interfacial Phenomena*, Academic Press, New York (1961).
2. D. Bedeaux, Non-equilibrium thermodynamics and statistical physics of the liquid–vapour interface, *Lect. Notes Phys.* **253,** 85–118 (1985).
3. D. Bedeaux, A. Albano and P. Mazur, Boundary conditions and non-equilibrium thermodynamics, *Physica* **82A,** 438–462 (1976).
4. F. Goodrich, The theory of capillary excess viscosities, *Proc. R. Soc. Lond. A*, **374,** 341–370 (1981).
5. T. S. Sorensen, Dynamics and instability of fluid interfaces, *Lect. Notes Phys.* **105,** 1–75 (1978).
6. D. A. Edwards, H. Brenner and T. Wasan, *Interfacial Transport Processes and Rheology*. Butterworth, New York (1991).
7. L. E. Scriven, Dynamics of a fluid interface (equation of motion for Newtonian surface fluids), *Chem. Engng Sci.* **12,** 98–108 (1960).
8. L. E. Scriven and C. V. Sternling, On cellar convection driven by surface-tension gradients: effects on mean surface tension and surface viscosity, *J. Fluid Mech.* **19,** 321–340 (1964).
9. P. Cardin and H.-C. Nataf, Nonlinear dynamical coupling observed near the threshold of convection in a two-layer system, *Europhys. Lett.* **14,** 655–660 (1991).
10. P. Cardin, H.-C. Nataf and P. Dewost, Thermal coupling in the layered convection: evidence for an interface viscosity control from mechanical experiments and marginal stability analysis, *J. Phys.* II *France* **1,** 599–622 (1991).
11. S. Wahal and A. Bose, Rayleigh–Bénard and interfacial instabilities in two immiscible liquid layers, *Phys. Fluids* **31,** 3502–3510 (1988).
12. G. Gousbet, J. Maquet, C. Rozé and R. Darrigo, Surface-tension and coupled buoyancy-driven instability in a horizontal fluid layer. Overstability and exchange of stability, *Phys. Fluids* **A2,** 903–911 (1990).
13. J. Maquet, G. Gousbet, A. Boîlemont, Numerical simulation of surface-tension and combined buoyancy-driven

convection in a liquid layer heated by a hot wire, *Int. J. Heat Mass Transfer* **35,** 2695–2703, 1992.
14. J. Earnshaw and A. McLaughlin, Waves at liquid surfaces—I and II, *Proc. R. Soc. Lond. A*, **433,** 663–678 (1991); **440,** 519–536 (1993).
15. H. Hühnerfuss, Hydrophilic hydration of monolayer molecules and its contribution to surface viscosity, *J. Colloid Interface Sci.* **126,** 384–385 (1988).
16. D. A. Nield, Surface tension and buoyancy effects in cellular convection, *J. Fluid Mech.* **19,** 341–352 (1964).
17. D. Villers and J. K. Platten, Influence of interfacial tension gradients on thermal convection in two superposed immiscible liquid layers, *Appl. Sci. Res.* **47,** 177–191 (1990).
18. A. G. Kirdyashkin, Thermogravitational and thermocapillary flows in a horizontal liquid layer under the conditions of a horizontal temperature gradient, *Int. J. Heat Mass Transfer* **27,** 1205–1218 (1984).
19. P. M. Parmentier, V. C. Regnier and G. Lebon, Buoyant-thermocapillary instabilities in medium-Prandtl-number fluid layers subjet to a horizontal temperature gradient, *Int. J. Heat Mass Transfer* **36,** 2417–2427 (1993).